

## Supplementary Information

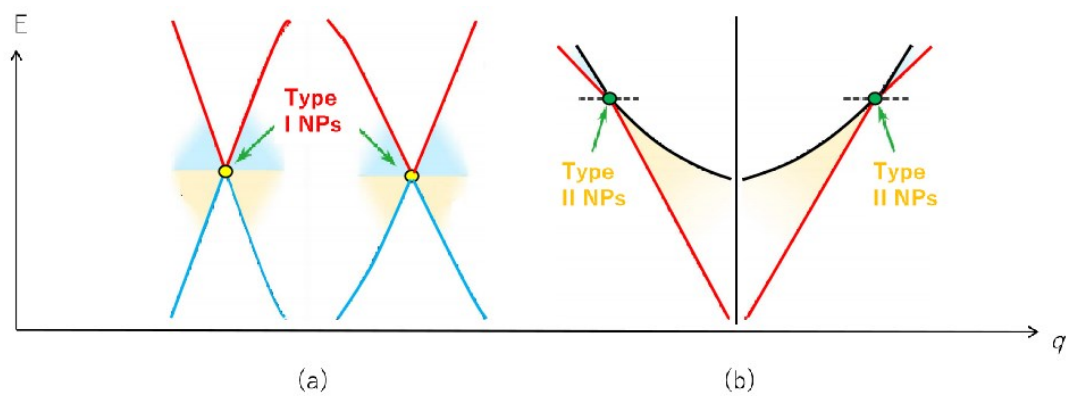


Fig. S1. Schematic diagrams of type I nodal points (a) and type II nodal points (b).

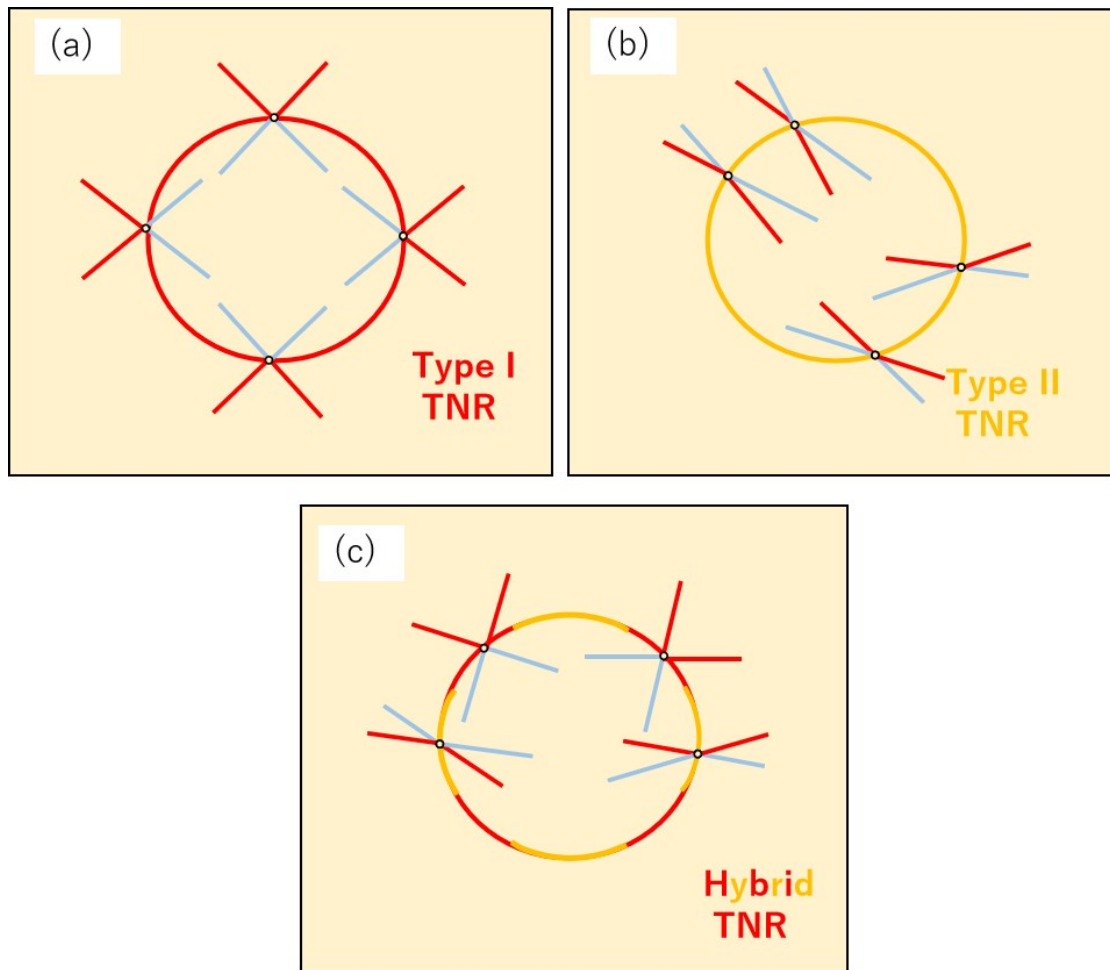


Fig. S2. Schematic diagrams of type I TNR (a), type II TNR (b) and hybrid-type TNR (c).

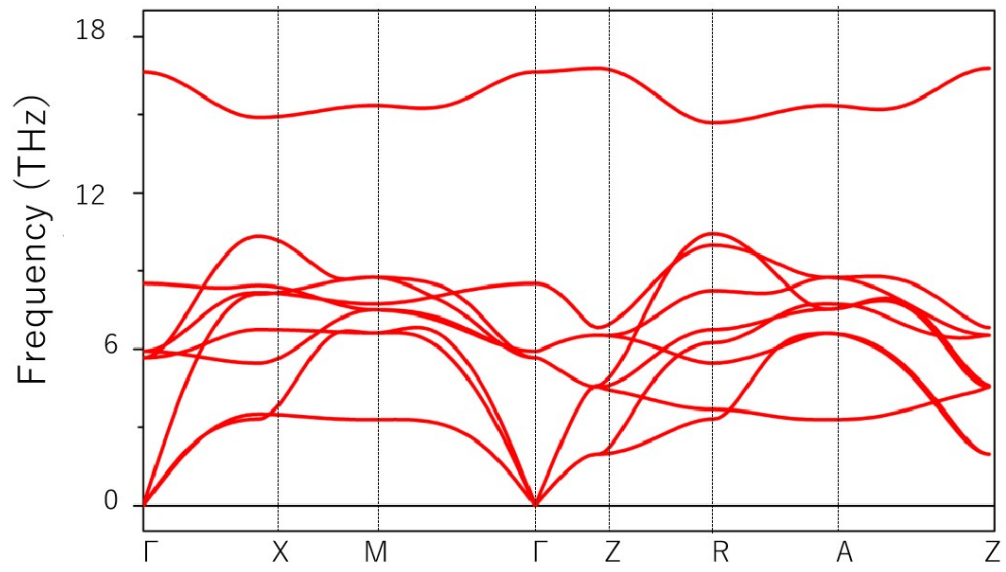


Fig. S3. Calculated phonon dispersion of quasi-2D  $\alpha$ -FeSi<sub>2</sub>.

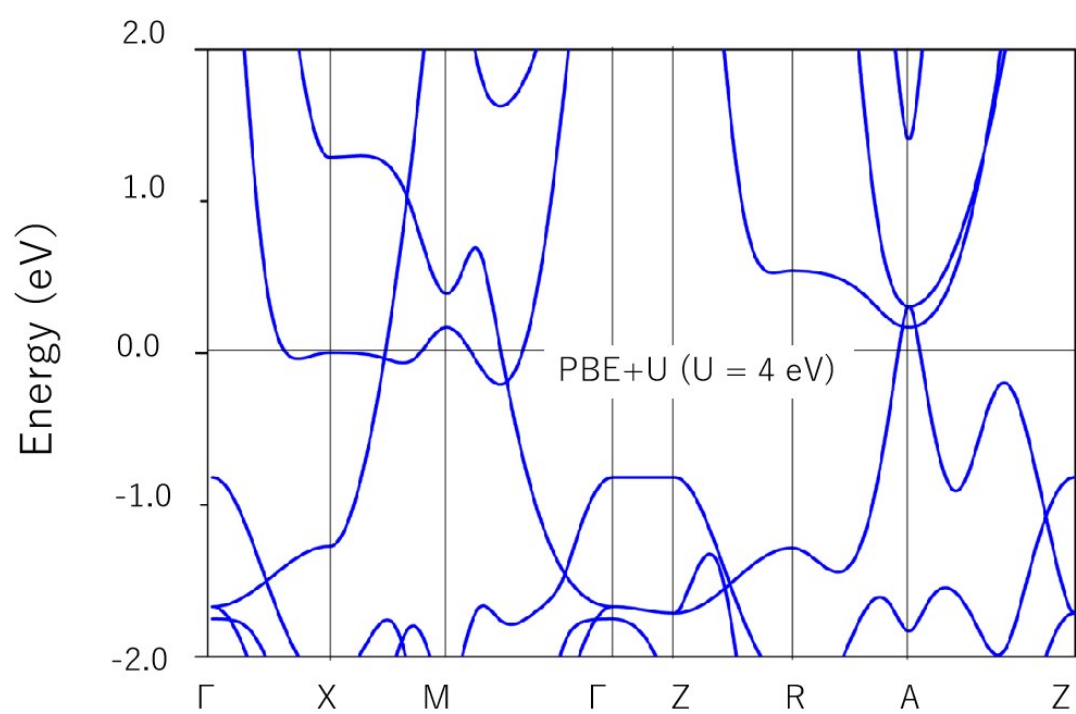


Fig. S4. Calculated band structure of quasi-2D  $\alpha$ -FeSi<sub>2</sub> with U = 4 eV for Fe - *d* orbitals.

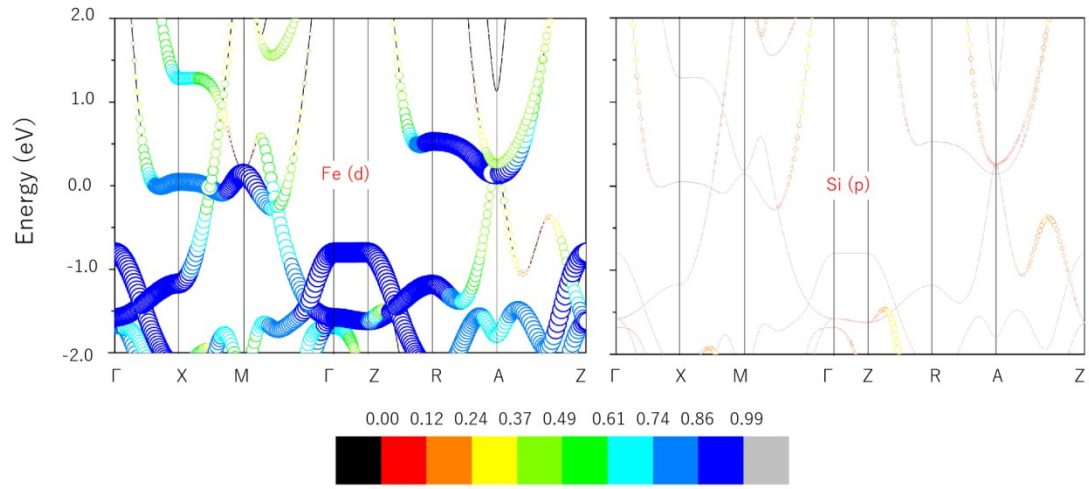


Fig. S5. Calculated orbital-resolved band structures of the Fe (*d*) and Si (*p*) orbitals for quasi-2D  $\alpha$ -FeSi<sub>2</sub>.

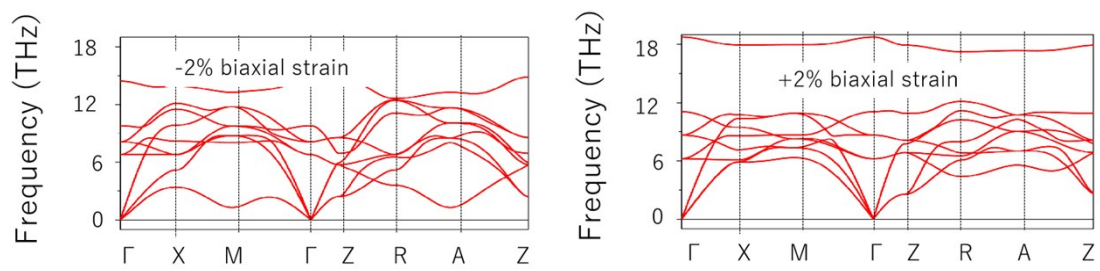


Fig. S6. Calculated phonon dispersions for quasi-2D  $\alpha$ -FeSi<sub>2</sub> under -2% and +2% biaxial strains.

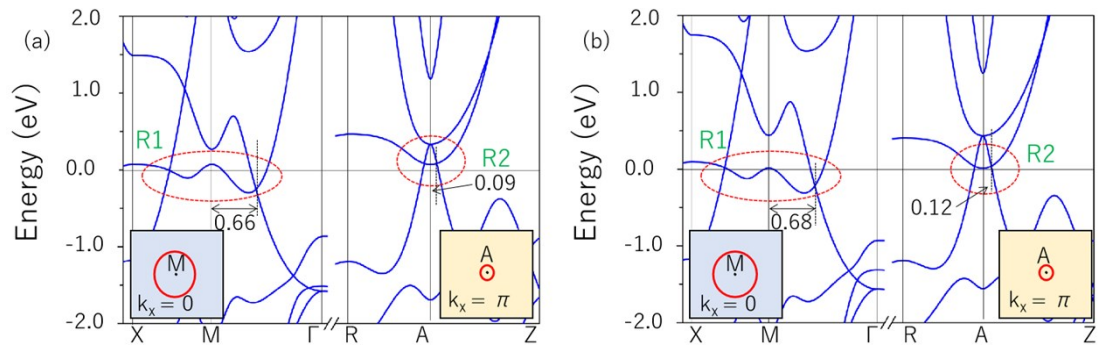


Fig. S7. Calculated band structures for quasi-2D  $\alpha$ -FeSi<sub>2</sub> under 1% and 2% biaxial strains.

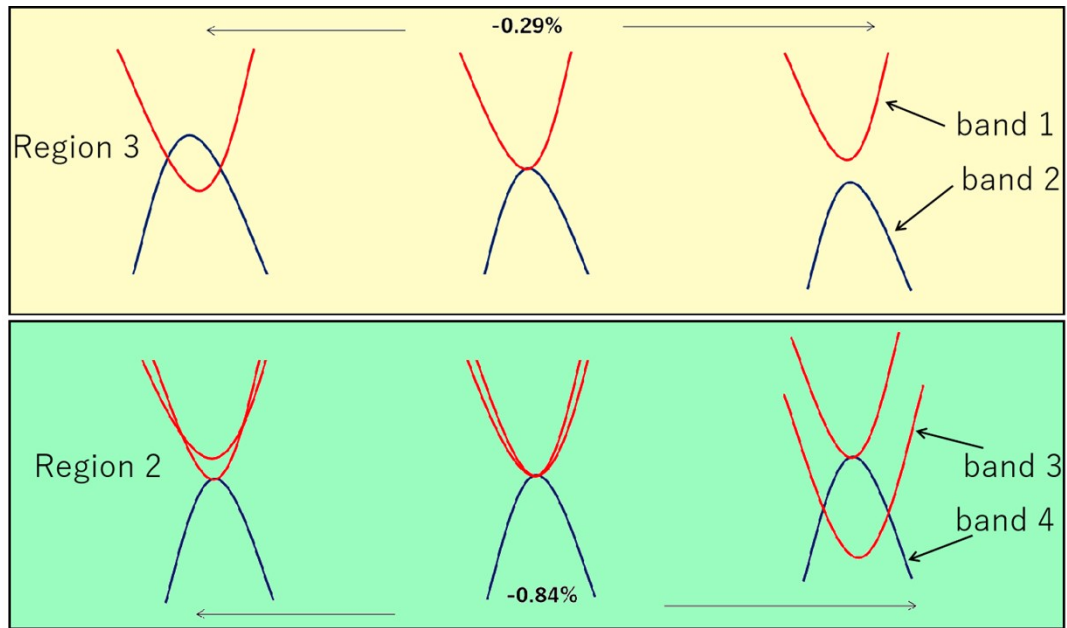


Fig. S8. Schematic diagrams of the changing of opposite-pockets-like bands near Fermi level in R3 and R2, respectively, in the range of -2% to +2% biaxial strain.



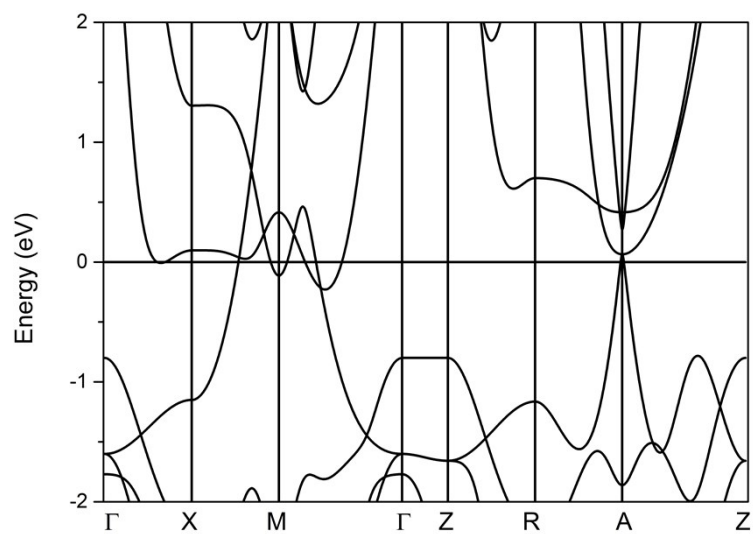


Figure S9: band structure of  $\alpha$ -FeSi<sub>2</sub> calculated by TPSS MGGA method at 0% strain.

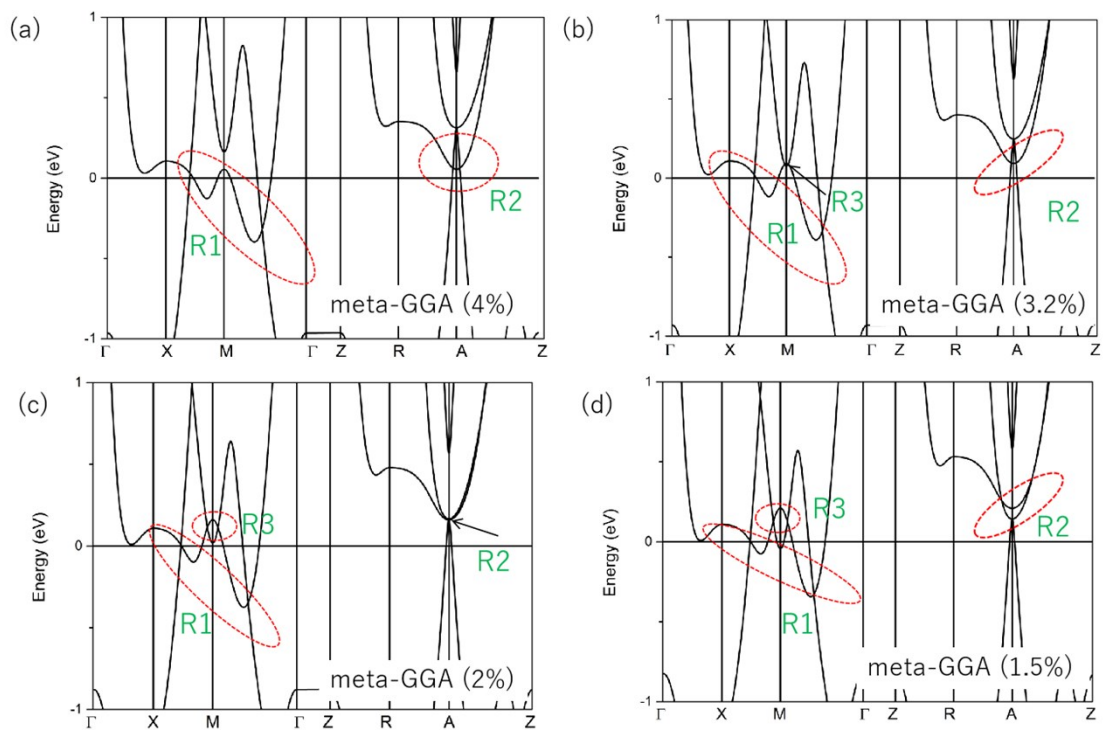


Figure S10: calculated band structures of  $\alpha$ -FeSi<sub>2</sub> calculated by TPSS MGGA method at different strains.